Azobenzene-Containing Liquid Crystal Triblock Copolymers: Synthesis, Characterization, and Self-Assembly Behavior

Wei Deng,[†,‡] Pierre-Antoine Albouy,[§] Emmanuelle Lacaze,[||] Patrick Keller,[‡] Xiaogong Wang,*[,†] and Min-Hui Li*[,‡]

Department of Chemical Engineering, School of Material Science and Engineering, Tsinghua University, Beijing, 100084, P. R. China; Institut Curie, CNRS UMR168, Laboratoire Physico-Chimie Curie, 26 rue d'Ulm, 75248 Paris Cedex 05, France; Laboratoire de Physique des Solides, CNRS UMR 8502, Université Paris-Sud, Bâtiment 510, 91405 Orsay Cedex, France; and Institut des Nano-Sciences de Paris, CNRS-UMR7588, Universités Pierre et Marie Curie-Paris 6 & Denis Diderot-Paris 7, 140 rue de Lourmel, 75015 Paris, France

Received November 21, 2007; Revised Manuscript Received January 21, 2008

ABSTRACT: A series of azobenzene-containing isotropic/nematic/isotropic liquid crystal (LC) triblock copolymers (PBMA-*b*-PMAazo444-*b*-PBMA) with different block ratios was synthesized by atom transfer radical polymerization (ATRP). The central block PMAazo444 is an azobenzene-containing side-on nematic liquid crystalline polymer and PBMA a coil polymer. These azo-triblock copolymers were prepared and studied with the aim of producing, in the future, photoresponsive elastomers with lamellar structure. Kinetic studies on the polymerization of the azobenzene-containing LC monomer demonstrate that its polymerization is a controlled process. A LC homopolymer with narrow molecular weight distribution ($M_w/M_n = 1.13$) was used as a difunctional macroinitiator to prepare the triblock copolymers by ATRP. The triblock copolymers were characterized by NMR, SEC, DSC, and POM. A triblock copolymer with 47 wt % of LC part self-assembles into a lamellar phase as evidenced both by SAXS and by TEM. The surface alignment of this lamellar phase on a silicon substrate was studied by AFM and compared with its nonphotosensitive triblock homologue (PBA-*b*-PA444-*b*-PBA). For this nonphotosensitive triblock copolymer the lamellas aligned parallel to the substrate, while for the azobenzene-containing triblock copolymer they organized perpendicular to the substrate.

Introduction

Block copolymers composed of both liquid crystalline (LC) and isotropic blocks are attractive candidates for the development of new functional materials, such as smart or responsive materials and electrooptical systems, because the block copolymers tend to self-assemble into ordered micro- or nanometer sized domains,[1] while special functionalities can be introduced via the liquid crystalline parts into the micro- or nanostructures.[2] In our previous work,[3] we have reported an "artificial muscle" elastomer made from a lamellar assembly of an isotropic/nematic/isotropic triblock copolymer, according to the model proposed by de Gennes.[4] The motor for the contraction/elongation is the reversible macromolecular backbone shape change, from stretched to spherical, that occurs at the thermal nematic to isotropic phase transition in side-on LC polymer blocks. Any polymer chain shape change induced by the disorganization or reorganization of LC mesogens, triggered by any stimulus, could be used as the motor for contraction in LC elastomers.[5] It is thus possible to produce elastomers responsive to other stimuli such as light, mimicking the phenomenon that occurs at the thermal nematic-to-isotropic transition. Such photoresponsive materials, with a fast photochemically induced contraction triggered by UV light, have been prepared successfully by several groups.[6–9] Our system was based on a network of azobenzene-containing LC homopolymers. Azobenzene chromophores can undergo reversible trans–cis isomerization under UV or visible light irradiation. The rodlike *trans*-azobenzene moieties are liquid crystalline, while the bent *cis*-azobenzene moieties are not mesomorphic and will act as impurities. As a consequence, the trans–cis isomerization of azobenzene will lower the nematic−isotropic phase transition temperature and induce a nematic–isotropic transition at the given temperature. Beside this promising photomechanical effect, azo-containing materials have also been developed for various applications such as holographic optical storage[10–14] or surface relief gratings.[15–17]

One of the long-term motivations of the research work pursued in our laboratories is to prepare photoresponsive elastomers with lamellar structures, since this striated structure should be more robust mechanically.[4] Therefore, the preparation of potentially photoresponsive block copolymers which display a lamellar organization is a key step toward this goal and is addressed in this paper. The second motivation of the present work was to explore the possibility to align a thin film of the side-on LC triblock copolymer using an interface. The microphase segregation (nanostructure formation) of block copolymers in thin film might bring the possibility to make patterned surfaces with even smaller feature sizes than those obtained by photolithography.[18,19] The well-aligned nanostructures of the LC triblock copolymers in thin film could also be used to produce micro- or nanoactuators on surface, e.g., active surface.[20] We report here on the synthesis, via atom transfer radical polymerization (ATRP), and liquid crystalline properties of a series of new isotropic/nematic/isotropic triblock copolymers, in which an azobenzene-containing side-on liquid crystalline polymer was used as central block (see Figure 1). The mesomorphic properties and self-assembled structures of the azo-triblock copolymers in bulk were studied by polarizing optical microscopy (POM), DSC, X-ray scattering, and TEM. With AFM, we also studied the orientation of two isotropic/nematic/isotropic LC triblock copolymers by an interface.

* Corresponding authors: Tel 86 10 62784561, Fax 86 10 62770304, wxg-dce@mail.tsinghua.edu.cn (X.W.); Tel 33 1 42346763, Fax 33 1 40510636, e-mail min-hui.li@curie.fr (M.H.L.).
[†] Tsinghua University.
[‡] Institut Curie, CNRS UMR168.
[§] Université Paris-Sud.
[||] Universités Pierre et Marie Curie-Paris 6 & Denis Diderot-Paris 7.

10.1021/ma702590j CCC: $40.75
Published on Web 03/07/2008

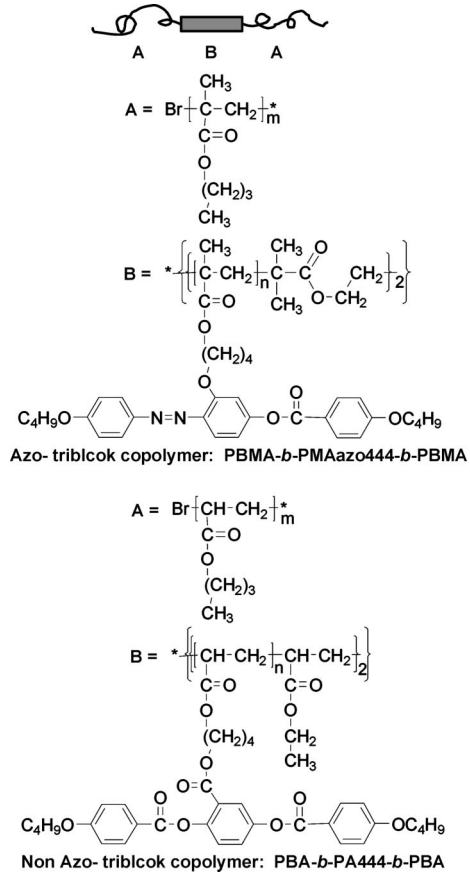

Figure 1. Chemical structures of the azo-triblock copolymer PBMA-*b*-PMAazo444-*b*-PBMA and the non-azo-triblock copolymer PBA-*b*-PA444-*b*-PBA.

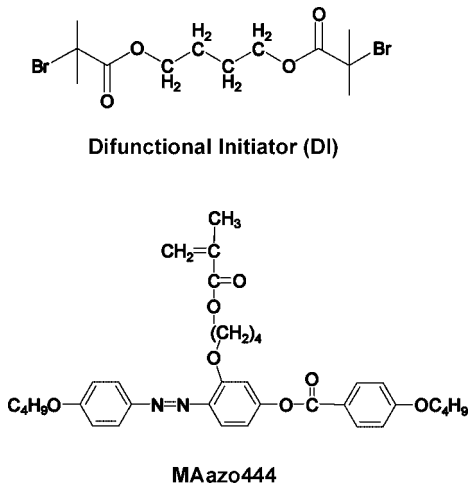

Figure 2. Chemical structures of ATRP initiator and azobenzene-containing LC monomer.

Experimental Section

1. Materials. The catalyst $Cu^{I}Br$ (98%, Aldrich) was purified as described previously.[22] Ligand 4,4′-di(*n*-nonyl)-2,2′-bipyridine (bpy9) (Aldrich) was purified by crystallization from absolute ethanol. Monomer *n*-butyl methacrylate (*n*-BMA) (99%, Aldrich) was filtered through a short column of neutral Al_2O_3 before use. Other chemical reagents were used without further purification. The solvents used were stored over 5 Å molecular sieves.

The difunctional initiator (DI), butan-1,4-bis(2-bromoisobutyrate) (Figure 2), was prepared as follows. Butan-1,4-diol (2.25 g, 25 mmol), triethylamine (6.08 g, 60 mmol), and THF (100 mL) were added in a 250 mL flask with a stirring bar. After the flask was cooled in an ice–water bath, α-bromoisobutyryl bromide (13.80 g, 60 mmol) in 50 mL of THF was added dropwise. The reaction was continued at room temperature overnight. The reaction mixture was filtered and THF removed by rotary evaporation. The residue was dissolved in 150 mL of ethyl acetate and shaken with 200 mL of distilled water. The organic phase was dried over anhydrous magnesium sulfate, filtered, and evaporated to get crude solid. After two crystallizations from ethanol, 3.01 g of a white solid was obtained (yield 77%). ^{1}H NMR: δ 1.80–1.84 (m, 4H, $-CH_2CH_2CH_2CH_2-$), 1.93 (s, 12H, $-CH_3$), 4.21–4.25 (t, 4H, $-O-CH_2-$).

The monomer MAazo444 (Figure 2) was synthesized following the procedure described previously.[23]

The non-azo-triblock copolymer PBA-*b*-PA444-*b*-PBA (M_n = 33 200, M_w/M_n = 1.37, weight ratio of nematic block to isotropic block is 51/49) used in this study (Figure 1) was synthesized as described previously.[21] The nematic block PA444 has M_n = 17 000 (degree of polymerization = 27) and M_w/M_n = 1.03.

2. Synthesis of the Difunctional Central Block PMAazo444. A typical ATRP procedure was performed. $Cu^{I}Br$ (22.95 mg, 0.160 mmol), $Cu^{II}Br_2$ (3.57 mg, 0.016 mmol), bpy9 (143.62 mg, 0.352 mmol), initiator DI (31.04 mg, 0.080 mmol), and monomer MAazo444 (2.408 g, 4 mmol) ($[Cu^{I}Br]:[Cu^{II}Br_2]:[bpy9]:[DI]:[M]$ = 2:0.2:4.4:1:50) were added into a Schlenk-type flask. The flask was degassed by four vacuum−argon cycles. Toluene (4 mL), which was previous degassed by bubbling argon for at least 30 min, was then introduced into the flask using a syringe which was also purged by argon. The reaction was held at 40 °C. Aliquots were withdrawn periodically from the flask by syringes prepurged with argon for the determination of the reaction conversion. Conversion was measured gravimetrically. After the end of the reaction, 1 mL of toluene was added to the reaction solution. The mixture was then poured into a large volume of diethyl ether. The precipitated polymer was purified twice by dissolution in a small amount of toluene and precipitation into a large volume of diethyl ether (in volume, toluene:ether = 1:20). The red sticky product PMAazo444 was dried under vacuum at 50 °C for 2 days. ^{1}H NMR: δ_H ($CDCl_3$) 0.78–0.92 (m, $-CH_3$), 1.24–1.69 (m, $-CH_x-CH_2-CH_x-$), 3.83 (m, $-O-CH_2-$), 6.60–6.82, 7.58, 7.73, 7.90–7.99 (m, *ArH*).

3. Polymerization of *n*-BMA with Difunctional PMAazo444 as Macroinitiator. Typically, $Cu^{I}Cl$ (3.56 mg, 0.036 mmol), $Cu^{II}Br_2$ (0.80 mg, 0.0036 mmol), bpy9 (32.31 mg, 0.079 mmol), and macroinitiator PMAazo444 (343.53 mg, 0.018 mmol; M_n = 19K, M_w/M_n = 1.09) were added into a Schlenk-type flask. The flask was degassed by four vacuum−argon cycles. Then *n*-butyl methacrylate (570 μL, 3.6 mmol) and toluene (1.0 mL), which were predegassed by bubbling argon for at least 30 min ($[Cu^{I}Cl]:[Cu^{II}Br_2]:[bpy9]:[PMAazo4444]:[BMA]$ = 2:0.2:4.4:1:200), were introduced into the flask using a prepurged syringe. The reaction was held at 80 °C. Samples were taken out from the flask periodically by syringe prepurged with argon. After the reaction was stopped, 1 mL of toluene was added into the flask to dilute the solution. The resulting polymer solution was poured into a large volume of methanol. The precipitated polymer was purified twice by dissolution in a small amount of toluene and precipitation into a large volume of methanol (volume ratio of methanol/toluene was 20/1). The orange-red powder of PBMA-*b*-PMAazo444-*b*-PBMA was dried under vacuum at 50 °C for 2 days. The ^{1}H NMR spectrum is shown in Figure 3.

4. Characterization. The molecular weights and the molecular weight distributions of the homopolymer PMAazo444 were measured by size exclusion chromatography (SEC) using two Waters Styragel HR 5E columns, a Waters 410 differential refractometer, and a Waters 486 UV detector, on line with a Wyatt miniDAWN light scattering instrument. The light wavelength of the differential refractometer is 930 nm, and that of the light scattering detector is 690 nm. THF was used as the eluent at 1 mL/min. The differential refractive index increment dn/dc = 0.193 was measured separately

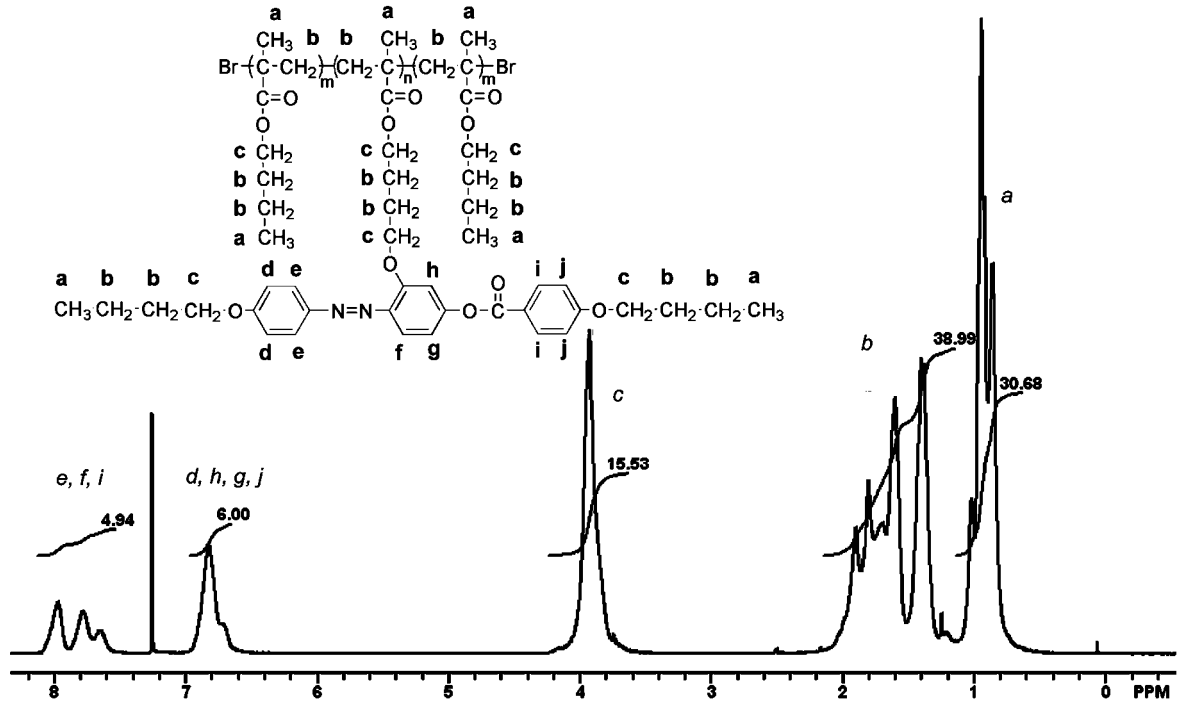

Figure 3. ^{1}H NMR spectra of the azo-triblock copolymer.

on the same refractometer (at $T = 40$ °C) for the homopolymer PMAazo444.

For the triblock copolymer, the molecular weight cannot be determined by SEC on line with the Wyatt miniDAWN light scattering instrument because the d*n*/d*c* changes with the block composition of the copolymers. So, the molecular weight distribution was estimated by the relative calibration method with polystyrene as standards. The molecular weight of PBMA block was calculated from ^{1}H NMR signals measured using a Bruker HW300 MHz spectrometer. Since the molecular weight of the central block is known by SEC, the ratio of the degree of polymerization (DP) of block PMAazo444 block to the DP of triblock copolymer can be deduced from the ratio between the integration of the aromatic signals ($\delta = 6.90$–8.06) in the LC central (A_{ar}) block and the integration of the signals of all terminal methyl groups ($\delta = 0.78$–0.92) in the triblock copolymer (A_{me}), as expressed in eqs 1 and 2.

$$(11x)/(9x + 6y) = A_{ar}/A_{me} \quad (1)$$

$$x + y = 1 \quad (2)$$

where x is the molar ratio of the azo monomer MAazo444 and y is the molar ratio of the monomer BMA.

The mesomorphic properties were studied by thermal optical polarizing microscopy using a Leitz Ortholux microscope equipped with a Mettler FP82 hot stage and differential scanning calorimetry using a Perkin-Elmer DSC7. The DSC7 instrument was calibrated with Perkin-Elmer indium calibration kit (mp: 429.78 K (156.60 °C); ΔH: 6.80 cal g^{-1}) for temperature and enthalpy changes. The heating and cooling rates were 10 °C min^{-1}.

5. Morphology Study by TEM. Samples for TEM experiments were prepared from a thick polymer film obtained by solution casting (film thickness: ~0.5–1 mm; polymer solution: 10 wt % in chloroform). The dried film was annealed at nematic temperature to allow microphase segregation, then embedded in epoxy resin, and ultramicrotomed at room temperature. The sections were stained with RuO_4 vapor and observed on a JEOL-JEM-1200EX electron microscope with an accelerating voltage of 100 kV.

6. Structural Study by X-ray Scattering. The X-ray scattering experiments were performed on fiber samples of polymers using Cu Kα radiation ($\lambda = 1.54$ Å) from a 1.5 kW rotating anode generator. Small-angle X-ray scattering (SAXS) and wide-angle X-ray scattering (WAXS) were performed separately. The fiber samples were drawn out from the molten polymers in nematic temperature. The diffraction patterns were recorded on photosensitive imaging plates.

7. Substrate Surface Alignment Study by AFM. The samples in $CHCl_3$ solution (10 g/L) were spin-casted on silicon wafers pretreated by a mixture (3/1 by volume) of concentrated sulfuric acid and hydrogen peroxide (30% in water) for 8 h. The films were then annealed at a temperature slightly below the nematic–isotropic transition temperature for 3 days. AFM experiments were performed on a Nanoscope 3100 (Veeco) in tapping mode with commercial silicon tips (radius is around 100 nm).

Results and Discussion

1. Polymerization Results. Atom transfer radical polymerization (ATRP) was chosen to prepare the azobenzene-containing LC triblock copolymers ABA. The LC central block, B, was first synthesized using a difunctional initiator. The block B was then used as difunctional macroinitiator in the polymerization of the two side blocks, A. In our previous work, we synthesized and studied non-azo-triblock copolymers PBA-*b*-PA444-*b*-PBA (Figure 1), in which the polymer backbones of the two blocks, PA444 and PBA, were polyacrylates. Polyacrylates were used rather than polymethacrylates because of the lower T_g. The thermoresponsive elastomers thus obtained were not brittle at ambient temperature. Thus, we first tried to synthesis azobenzene-containing nematic polyacrylate PAazo444 (polyacrylate equivalent of PMAazo444). For unclear reasons, ATRP as well as conventional radical polymerization of this azobenzene-containing nematic acrylate was not successful.[24] Recently, Forcén et al. reported an unsuccessful attempt to produce an azobenzene-containing methacrylate macroinitiator, using the CuCl/HMTETA/anisole system.[25] We successfully synthesized nematic polymethacrylates PMAazo444 by ATRP using improved procedures based on those described previously.[21,22] In order to control the molecular weight and the terminal functional groups, we made a preliminary kinetic study on the ATRP of MAazo444 using a difunctional initiator (see Figure 2). The results are presented in Table 1, Figure 4, and

Table 1. Homopolymers PMAazo444 Synthesized by ATRP

PMAazo444 sample	time (min)	conversion (%)	M_n[a]	M_w[a]	M_w/M_n[a]
P1	30	8	20 800	22 300	1.07
P2	60	33	23 900	25 100	1.05
P3	90	53	26 900	29 300	1.09
P4	120	66	28 100	31 800	1.13
P5	150	78	30 400	35 000	1.15

[a] Absolute molecular weight measured by the light scattering on line with SEC.

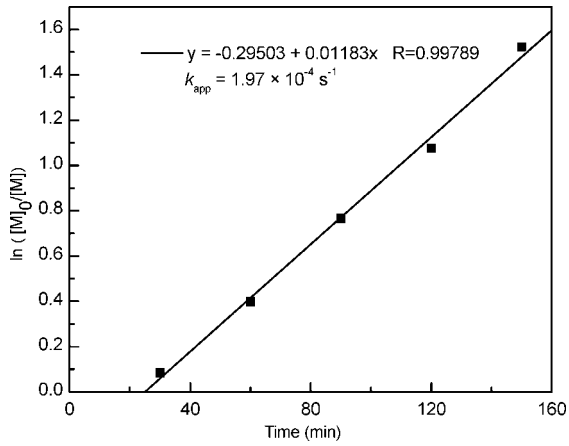

Figure 4. Kinetic plots for the ATRP of MAazo444 at 40 °C in toluene solution. The concentrations are $[MAazo444]_0 = 1.0$ M, $[DI]_0 = 0.02$ M, and $[Cu^IBr]/[Cu^{II}Br_2]/[Bpy9]/[DI] = 2:0.2:4.4:1$.

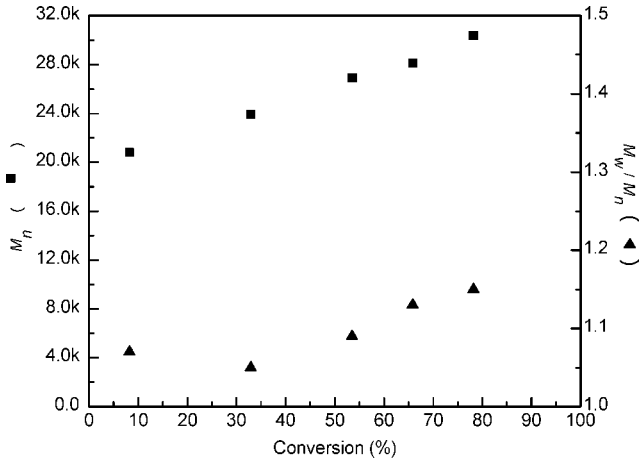

Figure 5. Molecular weight and polydispersity vs total conversion of LC monomer in the ATRP of MAazo444 at 40 °C in toluene solution. The concentrations are the same as for Figure 4.

Figure 5. Figure 4 shows a linear increase of $\ln[M]_0/[M]$ with time, and Figure 5 shows a linear increase of molecular weight with conversion. However, these two linear lines do not start from the origin. This might be tentatively explained by the following reason. In the purification procedure, diethyl ether was used as solvent for precipitation in order to remove all LC monomers that were not polymerized. However, diethyl ether could also dissolve low molecular weight polymers. Therefore, the conversion measured gravimetrically could be smaller than the real one at a given reaction time, while the molecular weight M_n could be greater than the average molecular weight of all polymers formed at this reaction time. Irreversible termination reactions at the very beginning of the polymerization might be another reason for the high experimental M_n values relative to the theoretical ones. Figure 5 shows low polydispersity values of around 1.1 for the obtained homopolymers. In conclusion, from this simple kinetic study we now know how to control

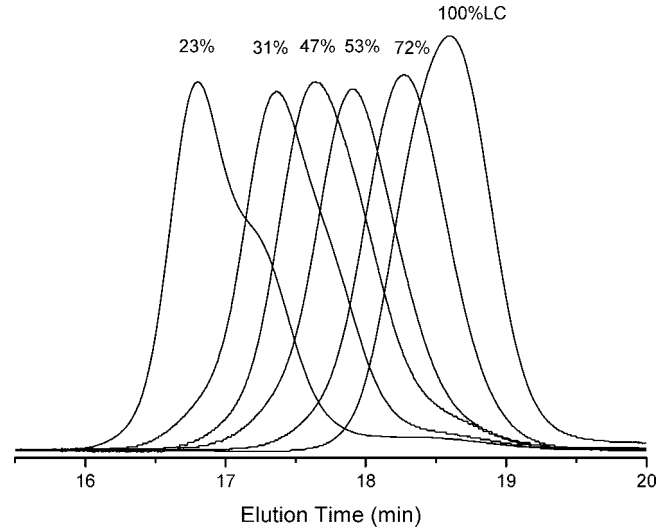

Figure 6. SEC chromatograms of the macroinitiator PMAazo444 and triblock copolymers PBMA-*b*-PMAazo444-*b*-PBMA (see Table 2 for data). The values noted above the curves indicate the weight ratio of the liquid crystalline block in the triblock copolymers.

empirically the polymerization of MAazo444 and obtain monodisperse PMAazo with a certain molecular weight.

We then used the above process to synthesize PMAazo444 functionalized at each end, keeping the conversion to around 50%. (The low conversion was chosen in order to minimize the chain termination between radicals and to ensure the end functionalities of PMAazo444.) The triblock copolymer PBMA-*b*-PMAazo444-*b*-PBMA was prepared by ATRP using this PMAazo444 as difunctional macroinitiator and *n*-butyl methacrylate as monomer. Cu^ICl was used as the catalyst.[26] In this mixed halogen system R−Br/Cu^ICl, halogen exchange occurred rapidly and gave faster initiation, slower propagation, and better control of molecular weight. The SEC chromatograms of the macroinitiator and five triblock copolymers synthesized are given in Figure 6. All SEC curves of the triblock copolymers are well separated from the peak of the macroinitiator toward shorter elution time (higher molecular weight), which means that all the macroinitiators were converted to triblock copolymers. The molecular weight distributions of the triblock copolymers were monomodal, except for Triblock5 (23% LC). The bimodality of Triblock5 (23% LC) might result from the coupling termination of two propagating chains, since longer reaction time was necessary for its synthesis. (By PS standard calibrated SEC, first peak corresponds to $M = 40$K, while the second shoulder peak corresponds to $M = 80$K). The reaction details and the characteristics (block ratios, molecular weights, and molecular weight distributions) of the triblock copolymers are listed in Table 2. A typical NMR spectrum is shown in Figure 3 for Triblock2.

2. Mesomorphic Properties and Self-Assembled Structures. The homopolymers PMAazo444 exhibit a nematic phase. The nematic–isotropic phase transition temperatures T_{NI} vary only slightly for samples with M_n in the range from 20 000 to 30 000. Phase transitions are Cr 73.5 N 93.8 I (10 °C/min) and I 92.1 N 58.5 g (−10 °C/min) for sample with $M_n = 20\,800$ and Cr 80.4 N 95.3 I (10 °C/min) and I 93.2 N 64.7 g (−10 °C/min) for sample with $M_n = 28\,100$. Schlieren-type textures were observed for nematic phase after annealing at a few degrees below T_{NI} for 24 h (see Figure 7a for POM picture).

DSC curves of the triblock copolymers are shown in Figure 8. In order to better observe the phase transitions upon heating, around 30 mg samples were used in the DSC experiments. The samples were first heated well above T_{NI}, followed by slow

Table 2. Triblock Copolymers PBMA-*b*-PMAazo444-PBMA Synthesized by ATRP Using Difunctional Homopolymer PMAazo444 as Macroinitiator

sample	$[BMA]_0/[PMAazo444]_0$[a]	reaction time (h)	conversion (%)[b]	M_n[c]	M_w/M_n[c]	M_n[d]	LC (wt %)[d]
PMAazo444				8 900	1.13	19 300[e]	100
Triblock1	100/1	1	53	12 300	1.17	26 800	72
Triblock2	200/1	2	60	18 100	1.19	35 700	54
Triblock3	200/1	8	77	22 700	1.20	41 100	47
Triblock4	350/1	4	86	29 700	1.29	62 300	31
Triblock5	500/1	21	91	49 100	1.33	83 900	23

[a] Feed ratio of monomer/macroinitiator. [b] Calculated by dividing the degree of polymerization of BMA in the result triblock copolymers to the feed ratio ($[BMA]_0/[PMAazo444]_0$). [c] Relative molecular weight(s) to PS standard calibration. [d] Calculated by the ^1H NMR. [e] Absolute molecular weight measured by the light scattering on line with SEC.

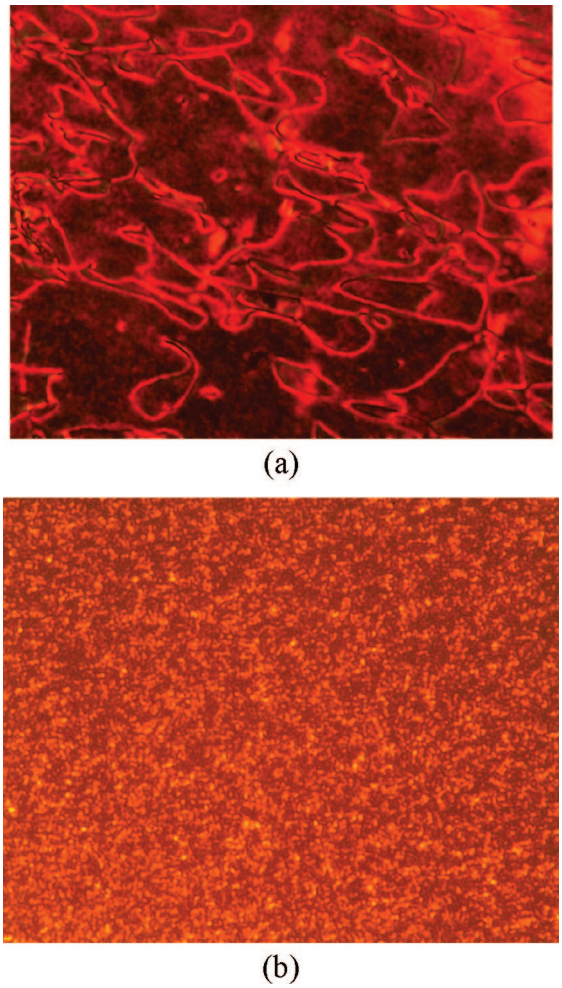

Figure 7. POM pictures showing the LC textures of the polymers: (a) homopolymer PMAazo444 P1 annealed at 92.6 °C for 24 h and (b) PBMA-*b*-PMAazo444-*b*-PBMA Triblock2 annealed at 65.0 °C for 24 h.

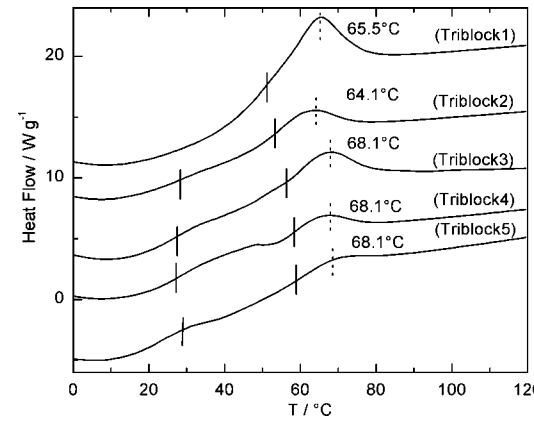

Figure 8. DSC thermograms of the five triblock copolymers PBMA-*b*-PMAazo444-*b*-PMBA upon heating at 40 °C/min (second heating scan after slow cooling from isotropic phase with cooling rate: –2 °C/min). The short lines on the curves indicate T_g, and the dotted lines indicate T_{NI}.

Table 3. Transition Temperatures of Triblock Copolymers PBMA-*b*-PMAazo444-PBMA Determined by DSC

sample	LC (wt %)	T_g (PBMA)	T_g (PMAzo444)	T_{NI}[a]	T_{IN}[b]
PMAazo444 (homopolymer)	100		62.8	96.1	92.7
Triblock1	72	–[c]	51.2	65.5	63.4
Triblock2	54	28.1	53.5	64.1	61.3
Triblock3	47	27.3	56.4	68.1	60.8
Triblock4	31	27.3	58.6	68.1	61.0
Triblock5	23	29.0	59.0	68.1	60.1

[a] Obtained from the second heating scan of the DSC thermograms of the polymers, which all own similar polymerization degree of liquid crystal part. After slow cooling from isotropic phase in −2 °C/ min, fast heating in 40 °C/ min. [b] Obtained from the second cooling scan, after fast heating in 40 °C/ min, and then cooling at 10 °C/ min. [c] Not detected.

cooling to −20 at −2 °C/min, and then fast heating to 120 at 40 °C/min. For Triblock1 with lowest contents of PBMA, the T_g of PBMA block was not detected. Cooling curves are not showed here, and the phase transition data are summarized in Table 3. A comparison between the DSC curves of the nematic central block PMAazo444 (macroinitiator) and a triblock copolymer PBMA-*b*-PMAazo444-*b*-PBMA is given in Figure 9. For all triblock copolymers, the transition temperatures from isotropic to nematic in the LC central block are lower than the T_{NI} of the equivalent LC homopolymer precursors. This situation is very similar to the one observed in non-azo-triblock polymers PBA-*b*-PA444-*b*-PBA.[21] The transition peaks for the azo-triblock copolymers PBMA-*b*-PMAazo444-*b*-PBMA are also much broader than for the LC homopolymer, especially upon heating. Those observations might be related to a relatively poorly defined interface between the nematic blocks and the isotropic blocks, the isotropic blocks playing the role of "impurities" toward the nematic mesophase. The azo-triblock copolymers PBMA-*b*-PMAazo444-*b*-PBMA are very viscous. Their textures are poorly defined even after annealing (see Figure 7b). The textures are not characteristic of any mesophase or self-assembled microsegregated phase.[27–29] So, the type of microsegregated phase needs to be determined by other structural studies such as X-ray diffraction and TEM.

Therefore, we performed SAXS and TEM studies on the sample PBMA-*b*-PMAazo444-*b*-PBMA Triblock3, which is likely to present a lamellar phase according to its block ratio (47% of LC). SAXS experiments were made on fiber samples at room temperature. The fiber samples were drawn from molten polymer in liquid crystalline state. Figure 10a shows the SAXS patterns of Triblock3 containing 47 wt % of LC block. The arrow in the figure indicates the fiber drawing direction. The semilogarithmic profile of SAXS signals is shown in Figure 10c, and three harmonies can be identified at position

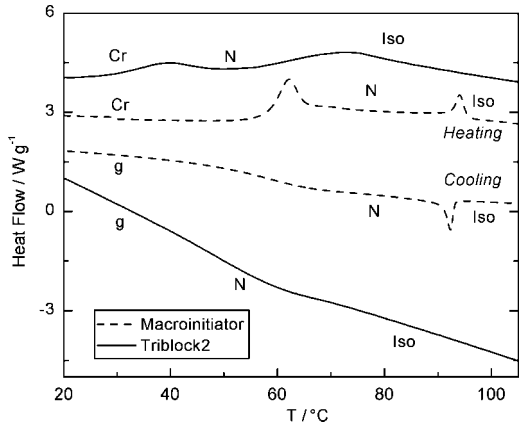

Figure 9. Comparaison of DSC thermograms of the macroinitiator PMAazo444 and Triblock2. First heating and cooling scan; scan rate: 10 °C/ min.

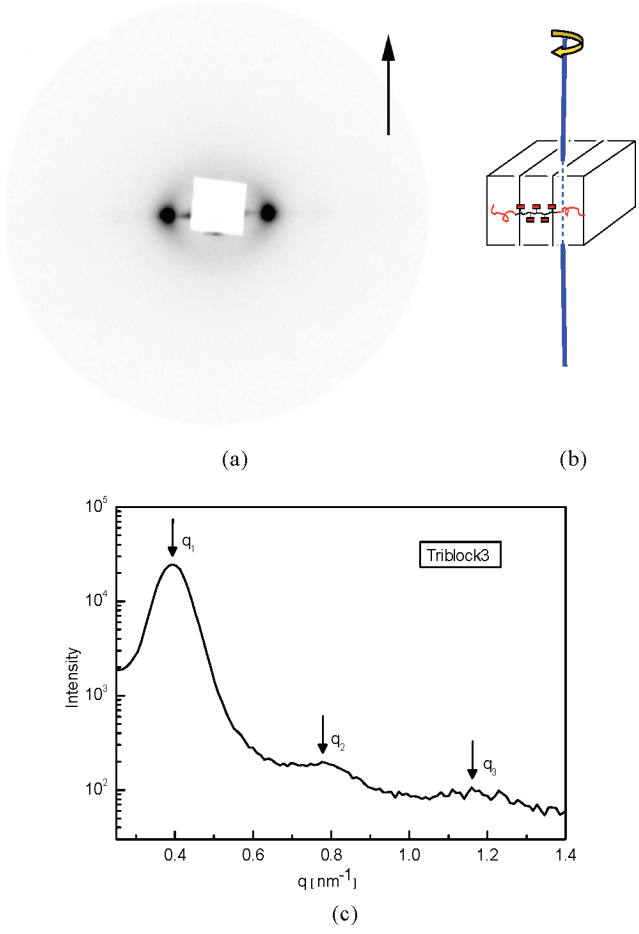

Figure 10. (a) SAXS pattern for fiber sample of Triblock3 at room temperature. The fiber sample was drawn from molten polymer, and the arrow indicates the fiber drawing direction. (b) Schematic representation of the triblock alignment in the fiber sample. (c) Semilogarithmic plot of the scattered intensity along equator vs the scattering vector q for the fiber sample of Triblock3, according to pattern (a). The arrows indicate the three orders of diffraction $q_1/q_2/q_3 = 1/2/3$. A lamellar microphase segregated morphology is then determined with lamellar spacing of 16 nm.

of $q_1/q_2/q_3 = 1/2/3$. This indicates clearly that Triblock3 (47%LC) self-assembles into a lamellar phase with lamellar spacing of 16 nm. This result was further supported on bulk

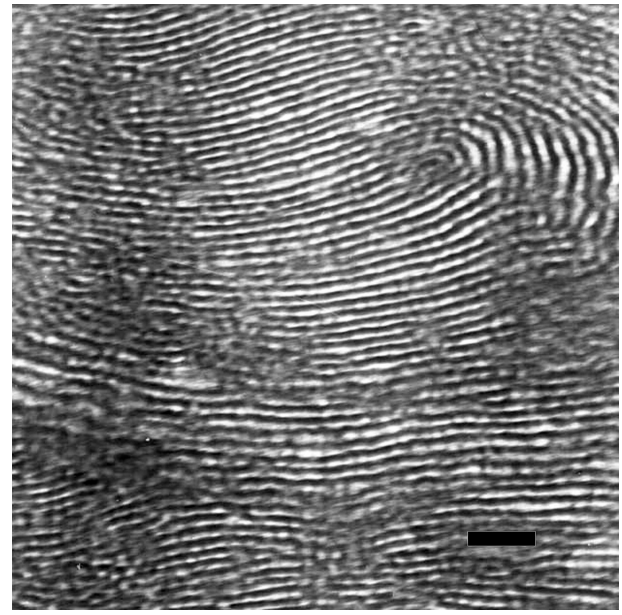

Figure 11. TEM image of Triblock3. The scale bar corresponds to 50 nm.

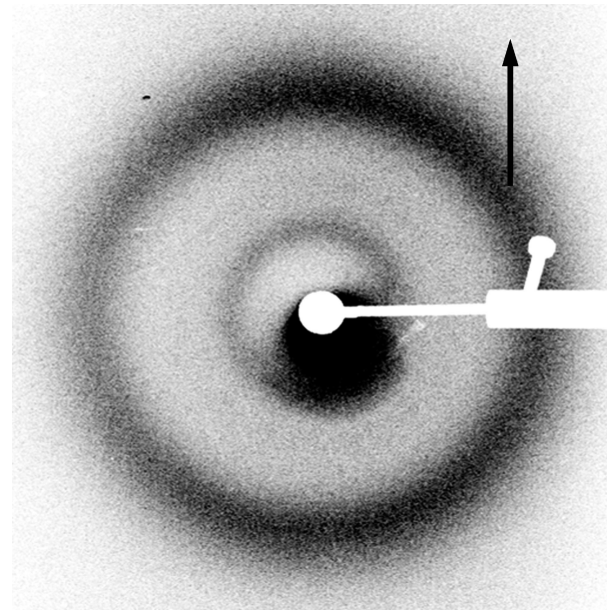

Figure 12. WAXS pattern for the fiber sample of Triblock3 at room temperature. The thick arrow indicates the fiber drawing direction. The diffuse diffraction ring corresponds to an average value of $2\pi/q = 0.48$ nm, which is the average distance between nematic mesogens. The diffuse ring is slightly intensified in the meridian direction. It means the mesogens rods are slightly aligned in the direction perpendicular to the fiber drawing direction.

samples by TEM. Clear lamellar structures were observed as shown in Figure 11.

Upon fiber drawing, the triblock copolymers align, with the layer normal perpendicular to the long axis of the fiber. However, the layer normal can be oriented along any direction in the plan perpendicular to the fiber long axis. Figure 12 shows the wide-angle X-ray scattering (WAXS) pattern of the same fiber sample Triblock3. The thick arrow indicates the fiber drawing direction. There is a diffuse diffraction ring in the WAXS pattern. It corresponds to an average value of $2\pi/q = 0.48$ nm, which is the average distance between nematic mesogens. From the pattern, the mesogens are aligned in a direction perpendicular to the fiber axis. Combining the results

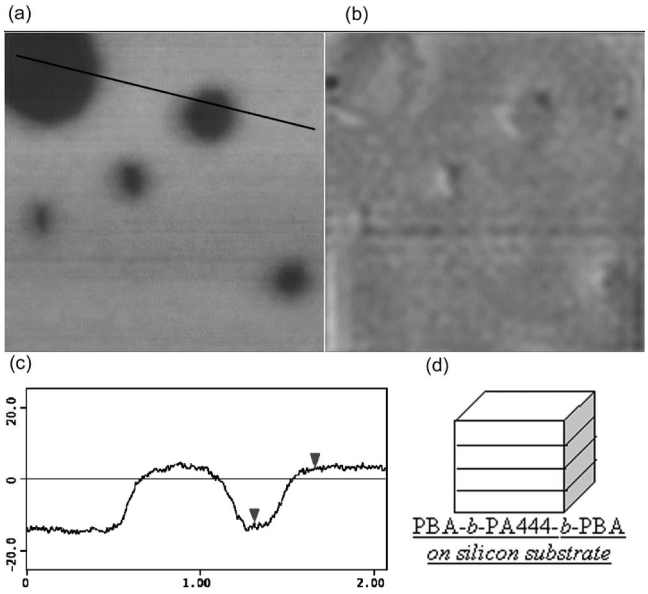

Figure 13. (a) Topography AFM image of PBA-*b*-PA444-*b*-PBA 51 wt % LC. Size: 2 μm × 2 μm (the vertical contrast is 50 nm). (b) Corresponding phase AFM image (the vertical contrast is 20°). (c) Height profile along the black line indicated in the height image (a). The vertical distance between the triangles is 16.7 nm. (d) Schematic representation of the alignment of corresponding triblock copolymer on silicon substrate.

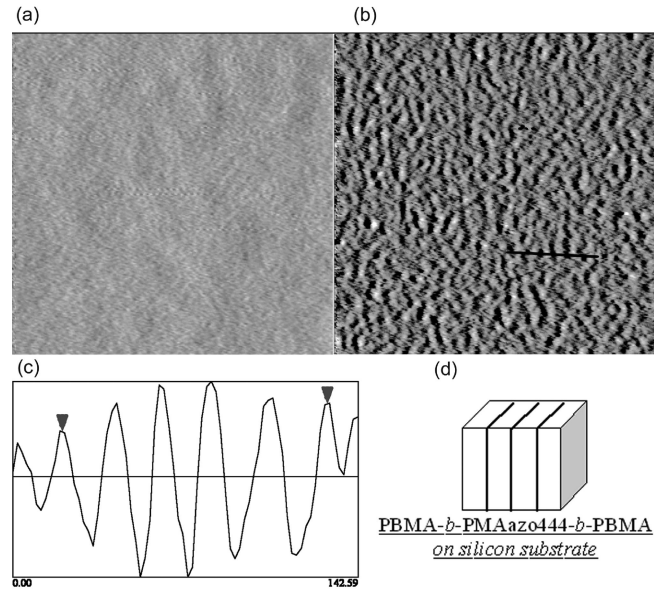

Figure 14. (a) AFM height image of PBMA-*b*-PMAazo444-*b*-PBMA 47 wt % LC (Triblock3), showing smooth surface. Size: 500 nm × 500 nm (the vertical contrast is 5 nm). (b) AFM phase image of PBMA-*b*-PMAazo444-*b*-PBMA 47 wt % LC (Triblock3). Size: 500 nm × 500 nm (the vertical contrast is 10°). (c) Phase profile along the black line indicated in the phase image (b). The horizontal distance between the triangles is 109.9 nm, leading to a distance between the heterogeneities in the phase image around 20 nm. (d) Schematic representation of the alignment of corresponding triblock copolymer on a silicon substrate.

from SAXS and WAXS, the alignments of lamellae and mesogens in the fiber samples are presented in Figure 10.

3. Substrate Surface Alignment of Triblock Copolymers with Lamellar Structure. By atomic force microscopy (AFM) we studied the alignment of a thin film of the side-on LC triblock copolymers on a substrate. Two isotropic/nematic/isotropic LC triblock copolymers, both of which self-assemble into lamellar nanostructures, were compared: the azo triblock copolymer (PBMA-*b*-PMAazo444-*b*-PBMA, Triblock3, 47 wt % LC, lamellar spacing $d = 16$ nm) and a non-azo-triblock copolymer (PBA-*b*-PA444-*b*-PBA, 51 wt % LC, lamellar spacing $d = 17$ nm). Silicon wafers were used as substrates. The film thicknesses ranged from 150 to 300 nm, as measured by AFM on scratched films, in agreement with the Newton tints of the samples.

Typical AFM images of the non-azo-triblock copolymer (PBA-*b*-PA444-*b*-PBA) are shown in Figure 13. The topography figure (height image) (Figure 13a) displays a flat surface with holes of depth around 17 nm (see the height profile in Figure 13c), a value close to the lamellar spacing of the lamellar phase, as measured by SAXS.[21,30] This result shows that the triblock copolymer is well-oriented with layers parallel to the silicon substrate, in agreement with the phase figure (Figure 13b) which displays no phase difference between the top surface and the interior of the holes, suggesting that the materials are similar in these two places. Different results were observed for the azo-triblock copolymer (Triblock3 47% LC). A typical height image is given in Figure 14a, which displays a rather smooth surface. The corresponding phase image is shown in Figure 14b and displays inhomogeneities which can be attributed to microphase separation at the surface. A typical distance between the heterogeneities is of the order of 20 nm (Figure 14c), which is close to the lamellar spacing (16 nm) of this triblock copolymer. For this triblock, the layers of the lamellar phase are oriented roughly perpendicular to the substrate. The different alignments of the two triblock copolymers on silicon substrate are represented schematically in Figure 13d and Figure 14d. These two very different organizations might come from the different polarities of azobenzene-containing mesogens and non-azo-mesogens, but other factors such as the different chemical structures of the polymer backbones (polyacrylate vs polymethacrylate) cannot be excluded.

Conclusion

We synthesized by ATRP a series of azobenzene-containing isotropic/nematic/isotropic LC triblock copolymers with different block ratios. With the aim of preparing in the future photoresponsive elastomers with lamellar structures, an azo side-on LC polymer was used, for the first time, as the central block. A triblock copolymer with 47 wt % of LC part self-assembles actually into lamellar phase as evidenced both by SAXS on fiber sample drawn from molten polymer and by TEM on bulk sample. In the fiber sample, the layer normal is in a plane perpendicular to the long axis of the fiber; in other words, the layer plans are parallel to the long axis. Surface alignment studies by AFM on thin films of this triblock copolymer revealed that the layer planes aligned perpendicular to the silicon substrate.

Cross-linkable azo-triblock copolymers with similar blocks compositions are now synthesized. Work is in progress in order to prepare aligned and cross-linked triblock azo-elastomers, which might be new photoresponsive "lamellar artificial muscles" elastomers.

Acknowledgment. We thank the French Embassy in China (Beijing) for the financial support to Wei Deng (Bourse doctorale en alternance 2004−2007). We thank M. J. Zhao (Department of Chemistry, Tsinghua University) for helpful discussions on ultramicrotome experiments and Heinz Amenitsch (Austrian SAXS beamline, Elettra Syncrotrone, Trieste, Italy) for his kind help.

References and Notes

(1) (a) Bates, F. S.; Fredrickson, G. H. *Phys. Today* **1999**, *52*, 32–38. (b) Hamley, I. W. In *Block Copolymers*; Oxford University Press: Oxford, England, 1999.
(2) Xie, P.; Zhang, R. *J. Mater. Chem.* **2005**, *15*, 2529–2550.

(3) Li, M. H.; Keller, P.; Yang, J. Y.; Albouy, P. A. *Adv. Mater.* **2004**, *16*, 1922–1925.
(4) De Gennes, P. G. *C. R. Acad. Sci. Paris, Ser. IIb* **1997**, *324*, 343–348.
(5) Li, M. H.; Keller, P. *Philos. Trans. R. Soc. London A* **2006**, *364*, 2763–2777.
(6) Finkelmann, H.; Nishikawa, E.; Pereira, G. G.; Warner, M. *Phys. Rev. Lett.* **2001**, *87*, 015501.
(7) Hogan, P. M.; Tajbakhsh, A. R.; Terentjev, E. M. *Phys. Rev. E* **2002**, *65*, 041720.
(8) Yu, Y.; Nakato, M.; Ikeda, T. *Nature (London)* **2003**, *425*, 145.
(9) Li, M. H.; Keller, P.; Li, B.; Wang, X. G.; Brunet, M. *Adv. Mater.* **2003**, *15*, 569–572.
(10) Eich, M.; Wendorff, J. H.; Reck, B.; Ringsdorf, H. *Macromol. Rapid Commun.* **1987**, *8*, 59–63.
(11) Kreuder, W.; Ringsdorf, H.; Herrmann-Schönherr, O.; Wendorff, J. H. *Angew. Chem., Int. Ed. Engl.* **1987**, *26*, 1249–1252.
(12) Breiner, T.; Kreger, K.; Hagen, R.; Häckel, M.; Kador, L.; Müller, A. H. E.; Kramer, E. J.; Schmidt, H. W. *Macromolecules* **2007**, *40*, 2100–2108.
(13) Häckel, M.; Kador, L.; Kropp, D.; Frenz, C.; Schmidt, H. W. *Adv. Funct. Mater.* **2005**, *15*, 1722–1727.
(14) Häckel, M.; Kador, L.; Kropp, D.; Schmidt, H. W. *Adv. Mater.* **2007**, *19*, 227–231.
(15) Natansohn, A.; Rochon, P. *Chem. Rev.* **2002**, *102*, 4139–4176.
(16) You, F. X.; Paik, M. Y.; Häckel, M.; Kador, L.; Kropp, D.; Schmidt, H. W.; Ober, C. K. *Adv. Funct. Mater.* **2006**, *16*, 1577–1581.
(17) Gao, J.; He, Y.; Xu, H.; Song, B.; Zhang, X.; Wang, Z.; Wang, X. G. *Chem. Mater.* **2007**, *19*, 14–17.
(18) Morikawa, Y.; Nagano, S.; Watanabe, K.; Kamata, K.; Iyoda, T.; Seki, T. *Adv. Mater.* **2006**, *18*, 883–886.
(19) Yu, H.; Iyoda, T.; Ikeda, T. *J. Am. Chem. Soc.* **2006**, *128*, 11010–11011.
(20) Buguin, A.; Li, M. H.; Silberzan, P.; Ladoux, B.; Keller, P. *J. Am. Chem. Soc.* **2006**, *128*, 1088–1089.
(21) Li, M. H.; Keller, P.; Albouy, P. A. *Macromolecules* **2003**, *36*, 2284–2292.
(22) Li, M. H.; Keller, P.; Grelet, E.; Auroy, P. *Macromol. Chem. Phys.* **2002**, *203*, 619–626.
(23) Li, M. H.; Auroy, P.; Keller, P. *Liq. Cryst.* **2000**, *27*, 1497–1502.
(24) After 3 days of reaction, the molecular weight of the polymer was so low that it could not precipitate from diethyl ether. In a recent publication some end-on azobenzene-containing polymers were obtained with low molecular weights after 1 week of reaction. See: Li, N.; Xu, Q.; Lu, J.; Xia, X.; Wang, L. *Macromol. Chem. Phys.* **2007**, *208*, 399–404.
(25) Forcén, P.; Oriol, L.; Sánchez, C.; Alcalá, R.; Hvilsted, S.; Jankova, K.; Loos, J. *J. Polym. Sci., Part A: Polym. Chem.* **2007**, *45*, 1899–1910.
(26) Shipp, D. A.; Wang, J. L.; Matyjaszewski, K. *Macromolecules* **1998**, *31*, 8005–8008.
(27) Hamley, I. W.; Castelletto, V.; Parras, P.; Lu, Z. B.; Imrie, C. T.; Itoh, T. *Soft Matter* **2005**, *1*, 355–363.
(28) Anthamatten, M.; Zheng, W. Y.; Hammond, P. T. *Macromolecules* **1999**, *32*, 4838–4848.
(29) Cui, L.; Zhao, Y.; Yavrian, A.; Galstian, T. *Macromolecules* **2003**, *36*, 8246–8252.
(30) Castelletto, V.; Parras, P.; Hamley, I. W.; Davidson, P.; Yang, J.; Keller, P.; Li, M. H. *Macromolecules* **2005**, *38*, 10736–10742.

MA702590J